Comparing two neurocognitive models of self-control during dietary decisions

Danielle Cosme*
Rita M. Ludwig*
Elliot T. Berkman

Department of Psychology, University of Oregon

*Author names in alphabetical order due to equal contribution

Number of words: 4961

Address correspondence to:
Danielle Cosme
Department of Psychology
1227 University of Oregon Eugene, OR 97403-1227
dcosme@uoregon.edu
541-346-5312

Abstract

Self-control is the process of favoring abstract, distal goals over concrete, proximal goals during decision making, and is an important factor in health and well-being. We directly compare two prominent neurocognitive models of human self-control with the goal of identifying which, if either, best describes behavioral and neural data of dietary decisions in a large sample of overweight and obese adults motivated to eat more healthfully. We extracted trial-by-trial estimates of neural activity during incentive-compatible choice from three brain regions implicated in self-control, dorsolateral prefrontal cortex, ventral striatum, and ventromedial prefrontal cortex, and assessed evidence for the dual-process and value-based choice models of self-control using multilevel modeling. Model comparison tests revealed that the value-based choice model outperformed the dual-process model, and best fit the observed data. These results advance scientific knowledge of the neurobiological mechanisms underlying self-control relevant decision making and are consistent with a value-based choice model of self-control.

Keywords: self-control, dual-process, value-based choice, health, decision neuroscience

Introduction

Self-control is central to health and well-being, and thus is a promising target for preventive interventions. Designing effective interventions requires a precise neurocognitive model self-control, but identifying a working model of self-control that maps onto underlying brain systems has proven challenging (Fujita, Carnevale, & Trope, 2018). One barrier to progress is that neural models of self-control are almost always tested in isolation, not directly compared to one another. Here, we define self-control as the process of favoring abstract, distal goals over concrete, proximal goals during decision making (Fujita, 2011), and compare two prominent neurocognitive models of self-control with the goal of identifying which best describes behavioral and neural data of dietary self-control relevant decisions, if either. The overarching purpose of this work is to develop a more-refined neurocognitive model of self-control to enable translational interventions to improve health outcomes.

We focus on two prominent models of self-control: dual-process models and value-based choice models. There are many variations on each class of models within the fields of social psychology and neuroeconomics; we draw hypotheses from the features that are most common within each model family. As such, it should be noted that the statistical models we compare in this paper are just several of many possible model instantiations. In general, dual-process models describe self-control as a battle between "hot" affective states (e.g., craving) and "cold" cognitive states (e.g., inhibitory control). In these models, self-control outcomes are the product of an antagonistic, seesaw relationship between affect and cognitive control (Kotabe & Hofmann, 2015). Though the precise neural location of these states differs substantially across studies (Berkman, 2017), dorsolateral PFC (dlPFC) is posited as a key node for flexibly maintaining goal representations (Braver et al., 2009) and implementing cognitive control across

a variety of cognitively demanding tasks (Duncan, 2013; Miller & Cohen, 2001; MacDonald et al., 2000; Shenhav, Botvinick, & Cohen, 2013; Buhle et al., 2014). On the other hand, regions in the mesolimbic dopamine system, such as ventral striatum (VS), are posited as key nodes for reward processing (McClure et al., 2007). According to these models, "cold" regions inhibit activity in "hot" regions (Figner et al., 2010), and therefore the balance, or difference, between lateral and subcortical activity should predict self-control relevant outcomes (Lopez et al., 2017; Lopez et al., 2014; Heatherton & Wagner, 2011). This is because these regions are hypothesized to serve opposing functions during self-control relevant choices.

In value-based choice models, subjective value from a range of choice attributes are integrated into a single accumulated expected value (or utility) for each choice (Berkman et al., 2017). Attributes are not limited to just "hot" and "cold" – they contribute separately to an accumulation process rather than compete with each other directly. Evidence for choice options is accumulated over time until one choice reaches the threshold for enactment, determining behavior and therefore self-control relevant outcomes (Tusche & Hutcherson, 2018; Harris, Clithero, & Hutcherson, 2018). Although it's possible to classify outcomes as self-control "successes" or "failures" (c.f. Hare, Camerer, & Rangel, 2009), value-based choice models often focus on the weights assigned to choice attributes (e.g., taste and health) during decision making rather than the outcomes per se. This is because choices are a combination of both signal and noise, but with enough choices available, it is possible to estimate parameters for relevant choice attribute that are more stable and drive behavior in the long run. For example, even if an individual "fails" to exert self-control by choosing to eat an unhealthy snack, that specific choice may occur in the presence of a relative shift in the value of healthiness or tastiness, which may accumulate over time to impact the probability of selecting healthy foods overall.

In value-based choice models, dlPFC and VS are also implicated as important nodes during dietary decisions, but their relationship is not expected to be antagonistic. Instead, these regions are hypothesized to independently encode the subjective value (i.e., goal value) derived from different choice attributes relevant to the decision making process (e.g., health and taste of food options) that are ultimately integrated in ventromedial prefrontal cortex (vmPFC). Although dlPFC is expected to contain information about the subjective value of health while individuals with goals to eat healthfully make dietary decisions, it is unclear whether dlPFC computes goal values, implements cognitive control to modulate the value of health, or plays some other role (Plassman, O'Doherty, & Rangel, 2010; Shenhav, 2017). In any case, within the value-based choice framework, (a) dlPFC is expected to show increased activation to healthy foods, (b) VS is expected to show increased activation to tasty, unhealthy foods, and (c) both regions are expected to positively correlate with vmPFC. Notably, options that are tasty *and* healthy are expected to elicit activity in both dlPFC and VS. In contrast to dual-process models, which predict that the balance between dlPFC and VS predict self-control, value-based choice models theorize that self-control relevant choices should be recoverable from activity in vmPFC.

Although it remains unclear what precise role vmPFC plays in decision making and whether it may serve as a final common pathway for choice, it has been implicated in choice regardless of stimulus type (e.g., food or money) or motivation (Rangel & Hare, 2010; Hare et al., 2010; Hare, Camerer, & Rangel, 2009; for a meta-analyses, see Clithero & Rangel, 2013; Bartra, McGuire, & Kable, 2013), and is thought to serve functions such as contributing to the integration or comparison of value signals (Lim, O'Doherty, & Rangel, 2011; Padoa-Schioppa & Conen, 2017; Levy & Glimcher, 2012) or alternatively, the construction of integrated meaning of the self in context (Roy, Shohamy, & Wager, 2012) or situational processing (Lieberman et al.,

2019). Consequently, value-based choice models suggest that the choice that evokes the greatest activation in vmPFC is likely to be enacted, and activation in vmPFC is driven by inputs from regions such as dlPFC, VS, and potentially their interaction. However, in contrast to dual-process models, which imply that lateral prefrontal and subcortical regions should be negatively correlated during decision making, value-based choice models posit that there is not necessarily a directional relationship between neural activity in brain regions representing the subjective value of choice attributes, which are subsequently integrated in vmPFC (i.e., these value signal inputs might be positively, negatively, or not related).

Despite these different predictions about how neural activity in dlPFC, VS, and vmPFC relate to self-control relevant decisions, these predictions are rarely compared within the same study. Researchers typically test the neural predictions of dual-process (Lopez et al., 2017) and value-based choice models (Hare, Camerer, & Rangel, 2009; Hare, Malmaud, & Rangel, 2011) separately, with notably few attempts to directly compare the models (Hutcherson, Plassmann, & Rangel, 2012). This may be because traditional univariate analyses are not well suited to model comparison.

Here, we employ a trial-by-trial modeling approach that allows us to relate neural activity to self-control relevant decisions in the dieting domain on a finer time scale than has previously been possible, and provides relative model fit indices. We recruited a large sample of overweight and obese participants (N = 94; BMI M = 31.33, BMI SD = 3.95) who had explicit dieting goals and examined neural responses in three brain regions of interest (ROIs) – dlPFC, VS, and vmPFC – while they made real dietary decisions about healthy and unhealthy snack foods during a food auction task (Hutcherson, Plassmann, & Rangel, 2012). Because participants enrolled in this study to improve healthy eating habits, there is an implicit self control dilemma between

distal health goals and proximal hedonic goals during the task. On each trial, we extracted the average blood-oxygenation-level dependent (BOLD) signal within each ROI, regressed bid value on these BOLD signal estimates, and assessed the relative evidence for each model of self-control using multilevel modeling. Dual-process models predict an association between the balance between activity in dlPFC and VS with bid value, whereas value-based choice models predict that vmPFC should be associated with bid value, even when dlPFC and VS are included in the statistical model. Our primary hypotheses and related analytic decisions were preregistered and are available in Supplementary material and online: https://osf.io/8bvxe/registrations.

Methods

Participants

Participants were 94 adults ages 35-46, (77 females, 16 males, 1 declined to respond; age M = 39.2, age SD = 3.5) with goals to eat healthfully, recruited as part of a 6-month longitudinal intervention study to improve healthy eating habits during middle age. The present study is a secondary analysis of the data. The sample size was determined based on the power analysis accompanying the original grant application (7R21CA175241-03) and constrained by the grant budget and award period. The data were collected before participants were randomized into intervention groups. To ensure all participants shared a healthy eating goal, only interested participants who endorsed readiness to change their eating habits were enrolled. We excluded four participants: two due to excessive motion, one due to technical failure, and one due to an incidental finding, yielding a total of 90 participants for statistical analyses. This study was approved by the University of Oregon Institutional Review Board; all participants gave written informed consent and were compensated for their participation.

Food auction task

To measure individual subjective value of healthy and unhealthy snack foods, participants completed a willingness-to-pay task (Hutcherson, Plassmann, & Rangel, 2012; http://github.com/UOSAN/WTP/tree/chives) while undergoing functional neuroimaging. The task is an incentive-compatible economic auction in which participants view images of thirty healthy and thirty unhealthy snack foods and choose how much they are willing to pay for each item. Foods that are energy-dense, high-sugar, or contain processed or red meat were classified as unhealthy, whereas foods that are not energy dense, and are high-fiber, low-fat, and low-sugar were classified as healthy. Participants were endowed with $2.00 to buy a snack and were told that one trial would be randomly selected and enacted. Bids greater than or equal to a randomly selected bid resulted in the participant getting the snack, whereas lower bids resulted in participants receiving the money, but not the snack. The optimal strategy is to bid the true amount one is willing to pay for each item. The task utilized an event-related design (Figure 1) and food image order was randomized for each subject.

Figure 1. Task design. Each trial consisted of a four second snack food presentation, followed by a four second bid period. Snack foods were either healthy (e.g., carrot sticks) or unhealthy (e.g., candy). All trials ended with a jittered fixation cross presented for 3-6 seconds (M = 4.38s).

Neuroimaging data acquisition

Data were acquired using a 3T Siemens Skyra scanner at the University of Oregon's Lewis Center for Neuroimaging. High resolution anatomical volumes were acquired using a T1-weighted MP-RAGE pulse sequence and functional volumes were acquired using a T2*-weighted echo-planar sequence (voxel size = 2 mm^3). Scan parameters are listed in Supplementary material.

Neuroimaging data preprocessing and analysis

Neuroimaging data were preprocessed and analyzed using SPM12 (Wellcome Department of Cognitive Neurology; http://www.fil.ion.ucl.ac.uk/spm). For each participant, functional images were realigned, coregistered to the high-resolution anatomical image, unwarped to reduce susceptibility artifacts, and smoothed using a $2mm^3$ FWHM Gaussian smoothing kernel. First-level statistical analyses were conducted in native space. Each trial was entered in the model as a separate regressor (rather than grouped by condition). Trial duration was specified as the eight seconds from food image onset to fixation (see Figure 1). Realignment parameters were transformed into five motion regressors, including absolute displacement from the origin in Euclidean distance and the displacement derivative for both translation and rotation, and a single trash regressor for images with motion artifacts (e.g., striping) identified using automated motion assessment (Version v0.2-alpha; Cosme, Flournoy, & DeStasio, 2018) and visual inspection. These regressors were included as covariates of no interest. Two participants were excluded for having >10% unusable volumes, which was more than three standard deviations from the median (*Mdn* = 1.57%, *SD* = 3.21%). The resulting statistical maps for each trial were concatenated to create a beta-series (Rissman et al., 2004). Preprocessing and analysis scripts are available online (https://osf.io/pevmy).

ROI definition and parameter extraction

We defined bilateral ROIs for dlPFC, vmPFC, and VS (see Figure 2) using the Desikan-Killiany (Desikan et al., 2006) and Destrieux (Destrieux et al., 2010) cortical parcellation atlases and the FreeSurfer segmentation atlas (Fischl et al., 2002), and mapped these ROIs to participants' T1-weighted anatomical scans using FreeSurfer 6 (Fischl, 2012). To determine which cortical parcels to use, we inspected meta-analytic association test maps from NeuroSynth (Yarkoni et al., 2011) for the following terms: cognitive control, dlPFC, value, and vmPFC, and identified overlapping FreeSurfer parcels (see Supplementary materials, Figure S1). To create the dlPFC ROI, we concatenated the middle frontal gyrus and the inferior frontal sulcus parcels. We created the vmPFC ROI using the medial orbitofrontal cortex parcels and the VS ROI by concatenating the nucleus accumbens and putamen segments. All ROIs were concatenated and binarized using the fslmaths function in FSL 5.0.10 (Jenkinson et al., 2012) and resliced to $2mm^3$ using SPM12. This process yielded individually defined dlPFC, vmPFC, and VS ROIs for each participant. To calculate the mean BOLD signal across the voxels in each ROI, we use the 3dmaskave function in AFNI 18.2.04 (Cox, 1996). For each participant, we extracted the mean parameter estimate of BOLD signal within each ROI for each trial in the beta-series. To account for differences in variability between individuals and ROIs, parameter estimates were standardized within participant and ROI.

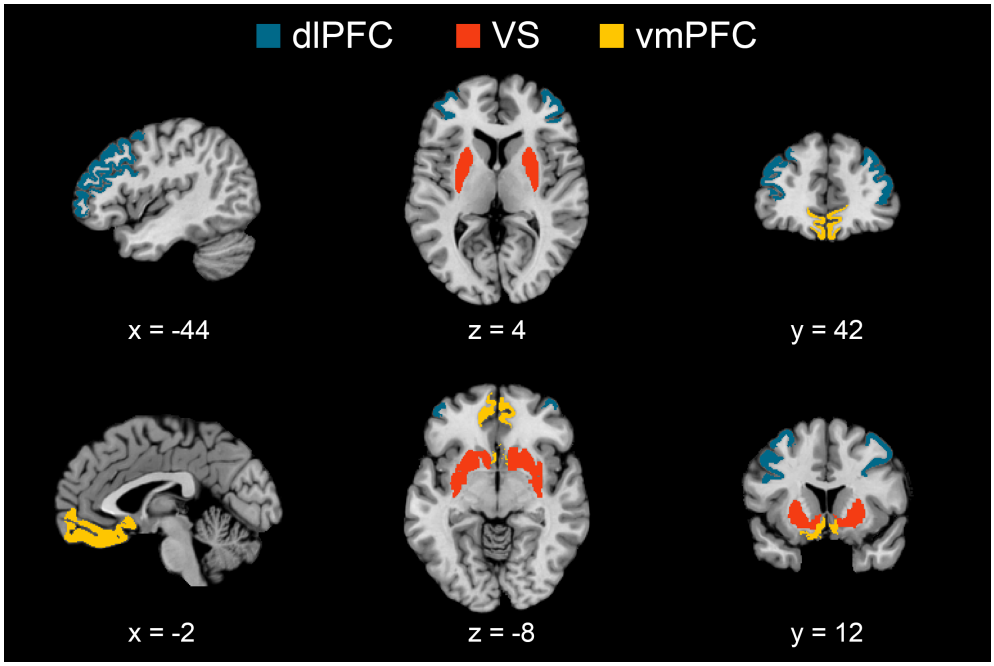

Figure 2. Regions of interest in volumetric space. dlPFC = dorsolateral prefrontal cortex, VS = ventral striatum, vmPFC = ventromedial prefrontal cortex.

Multilevel modeling

Evidence for the dual-process and value-based choice models of self-control was assessed by inspecting parameter estimates from a series of multilevel models. Statistical analyses were conducted in R 3.5.1. (R Core Team, 2018; https://www.r-project.org/) using the lme4 package (Bates et al., 2015). For each theoretical model, we compared a series of nested statistical models in which bid value was the criterion and neural predictors were added to a base model that included only the fixed effect of Food Type (healthy or unhealthy). For all models, only participant intercepts were treated as random effects. We compared nested models using chi-square difference tests; models were treated as significantly improving model fit if $p < .05$. To determine the best fitting model across theoretical models, we inspected the Akaike information criterion (AIC). Because AIC improves as the predictive value of a model increases (Aho, Derryberry, & Peterson, 2014), this comparison reveals which of the models maximizes accuracy in predicting bid value (where smaller AIC indicates better prediction accuracy). To

estimate multilevel model effect sizes, we calculated R^2 according to the guidelines in Lorah (2018). To estimate correlations between ROIs and account for the nested structure of trials within participants, we calculated repeated measures correlations using the rmcorr package (Bakdash & Marusich, 2017) in R. Because these models are only several of many possible ones, we also run additional, non-preregistered models and compared model fit using a specification curve (Simonsohn, Simmons, & Nelson, 2015). The results of this analysis can be found in Supplementary material.

Dual-process model comparison. To characterize the competitive nature of dlPFC and VS posited by the dual-process model, we created a "balance" score (Lopez et al., 2017) by subtracting estimates of activity in VS from dlPFC on each trial. Positive values indicate relatively greater dlPFC activity, whereas negative values indicate relatively greater VS activity. To test dual-process predictions, we compared model fit among the following models. As stated in our preregistration, if DP1 is the best fitting model and the balance score (dlPFC - VS) is significantly associated with bid value, we will interpret this as evidence for the dual-process model of self-control. However, if DP2 is the best fitting model, suggesting that vmPFC is significantly associated with bid value, we will interpret this as evidence for the value-based choice model, which is the only model that predicts a critical role for the vmPFC in self-control.

First level models:

Base model: Y_{ij} (Bid value of trial *i* by person *j*) = $\beta_{0j} + \beta_{1j}\text{Food Type}_{ij} + \varepsilon_{ij}$

DP1: Y_{ij} (Bid value of trial *i* by person *j*) = $\beta_{0j} + \beta_{1j}\text{Food Type}_{ij} + \beta_{2j}(\text{dlPFC}_{ij} - \text{VS}_{ij}) + \varepsilon_{ij}$

DP2: Y_{ij} (Bid value of trial *i* by person *j*) = $\beta_{0j} + \beta_{1j}\text{Food Type}_{ij} + \beta_{2j}(\text{dlPFC}_{ij} - \text{VS}_{ij}) + \beta_{3j}\text{vmPFC}_{ij} + \varepsilon_{ij}$

Second level equations:

$\beta_{0j} = \gamma_{00} + \mu_{0j}$

$\beta_{1j} = \gamma_{10}$

(In DP1 and DP2): $\beta_{2j} = \gamma_{20}$

(in DP2): $\beta_{3j} = \gamma_{30}$

Value-based choice model comparison. To assess evidence for this theoretical model, we compared the following statistical models. As stated in our preregistration, if VB1 – which specifies terms for dlPFC and VS to represent subjective value of relevant choice attributes and vmPFC as the value integrator – is the best fitting model and the neural predictors are significantly associated with bid value, we will interpret this as evidence for the value-based choice model. To mirror the model comparison for the dual-process models, we also planned to test whether adding the balance score (dlPFC - VS) to the model (VB2) would improve model fit. However, this model did not converge because the balance score is a linear combination of dlPFC and VS and was therefore inestimable.

First level equations:

Base model: Y_{ij} (Bid value of trial *i* by person *j*) = $\beta_{0j} + \beta_{1j}$Food Type$_{ij} + \varepsilon_{ij}$

VB1: Y_{ij} (Bid value of trial *i* by person *j*) = $\beta_{0j} + \beta_{1j}$Food Type$_{ij} + \beta_{2j}$dlPFC$_{ij} + \beta_{3j}$VS$_{ij} + \beta_{4j}$vmPFC$_{ij} + \varepsilon_{ij}$

VB2: Y_{ij} (Bid value of trial *i* by person *j*) = $\beta_{0j} + \beta_{1j}$Food Type$_{ij} + \beta_{2j}$dlPFC$_{ij} + \beta_{3j}$VS$_{ij} + \beta_{4j}$vmPFC$_{ij} + \beta_{5j}$(dlPFC$_{ij}$ - VS$_{ij}$) + ε_{ij}

Second level equations:

$\beta_{0j} = \gamma_{00} + \mu_{0j}$

$\beta_{1j} = \gamma_{10}$

(In VB1 and VB2): $\beta_{2j} = \gamma_{20}$

(In VB1 and VB2): $\beta_{3j} = \gamma_{30}$

(In VB1 and VB2): $\beta_{4j} = \gamma_{40}$

(In VB2): $\beta_{5j} = \gamma_{50}$

Value integration in vmPFC. The value-based choice model specifies that value signals from dlPFC and VS are integrated in vmPFC. To assess evidence for this hypothesis, we regressed trial-level vmPFC activity on dlPFC and VS activity and their interaction. Participant intercepts were modeled as random effects. We expected that if vmPFC integrates the value signals from dlPFC and VS, then the fixed main effects of each region on vmPFC activity would be significant and positive, and that the interaction between these regions also would be significantly associated with vmPFC activity.

First level equation:
VMPFC: Y_{ij} (vmPFC on trial *i* by person *j*) = $\beta_{0j} + \beta_{1j}dlPFC_{ij} + \beta_{2j}VS_{ij} + \beta_{3j}dlPFC_{ij} \times VS_{ij} + \varepsilon_{ij}$

Second level equations:
$\beta_{0j} = \gamma_{00} + \mu_{0j}$
$\beta_{1j} = \gamma_{10}$
$\beta_{2j} = \gamma_{20}$
$\beta_{3j} = \gamma_{30}$

Results

Descriptives

Inspection of the data revealed a main effect of the Food Type (healthy vs. unhealthy) on bid value, such that participants were willing to pay more for healthy foods than unhealthy foods (see Figure 3; $M_{healthy} = 0.96$, $SD_{healthy} = 0.65$; $M_{unhealthy} = 0.66$, $SD_{unhealthy} = 0.63$). This is not unexpected given the dieting goals of participants in the sample. Visual inspection of the neural data revealed moderate positive correlations among the ROIs (see Table 1). In terms of differential neural activation, healthy foods were associated with greater BOLD signal than unhealthy foods in dlPFC and VS, but not vmPFC (see Figure 4). In terms of behavioral responses, higher bid values were associated with increased BOLD signal in all ROIs (see Figure 5) and similar trajectories were observed for both healthy and unhealthy foods (see Figure 6). The relevant inferential tests are reported in the following section.

Table 1
Repeated Measures Correlations Among ROIs

ROI	*M*	*SD*	1	2	3
1. VS	0.82	1.10	–		
2. dlPFC	0.79	1.10	.52 [.50, .54]	–	
3. vmPFC	0.13	1.09	.35 [.33, .37]	.50 [.48, .52]	–

Note. N = 5,220 trials. All correlations are statistically significant, $p < .001$. 95% confidence intervals are bracketed. Correlations adjust for trials nested within participant using multilevel modeling.

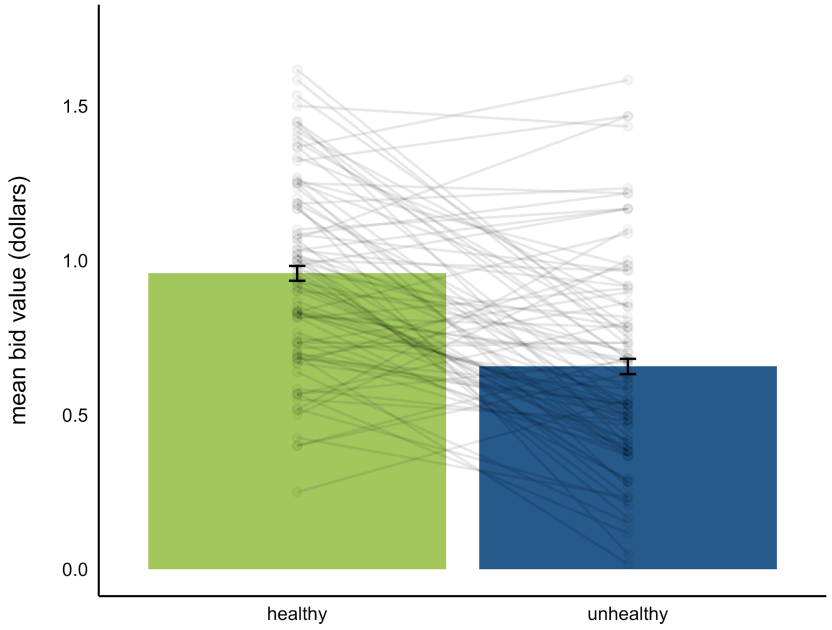

Figure 3. Mean bid value in dollars for healthy and unhealthy snack foods. Points represent mean bid value for individual participants. Error bars are 95% confidence intervals across trials.

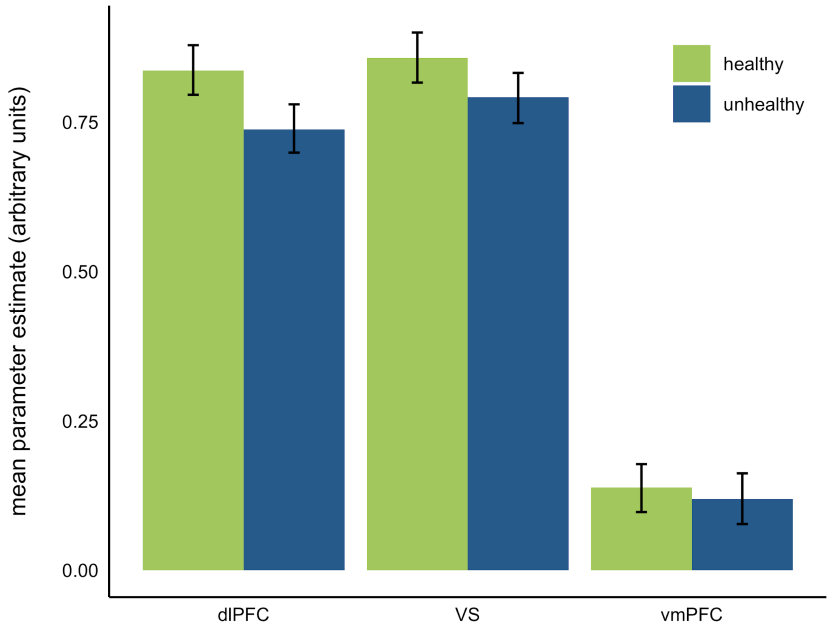

Figure 4. Mean parameter estimates of BOLD signal as a function of Food Type (healthy or unhealthy) and ROI. Error bars are 95% confidence intervals across trials. dlPFC = dorsolateral prefrontal cortex, VS = ventral striatum, vmPFC = ventromedial prefrontal cortex.

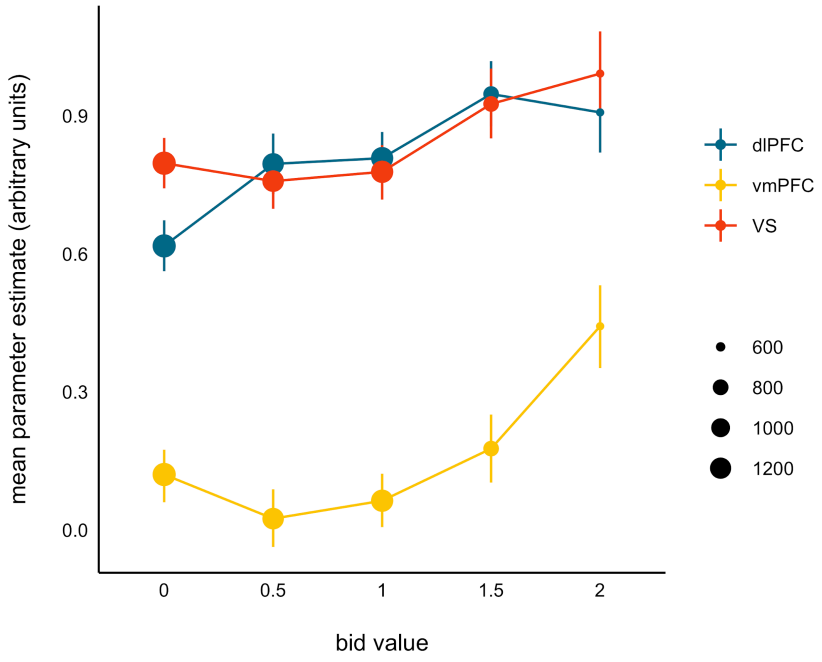

Figure 5. Mean parameter estimates of BOLD signal as a function of bid value and ROI. Points are scaled by the number of observations. Error bars are 95% confidence intervals across trials. dlPFC = dorsolateral prefrontal cortex, VS = ventral striatum, vmPFC = ventromedial prefrontal cortex.

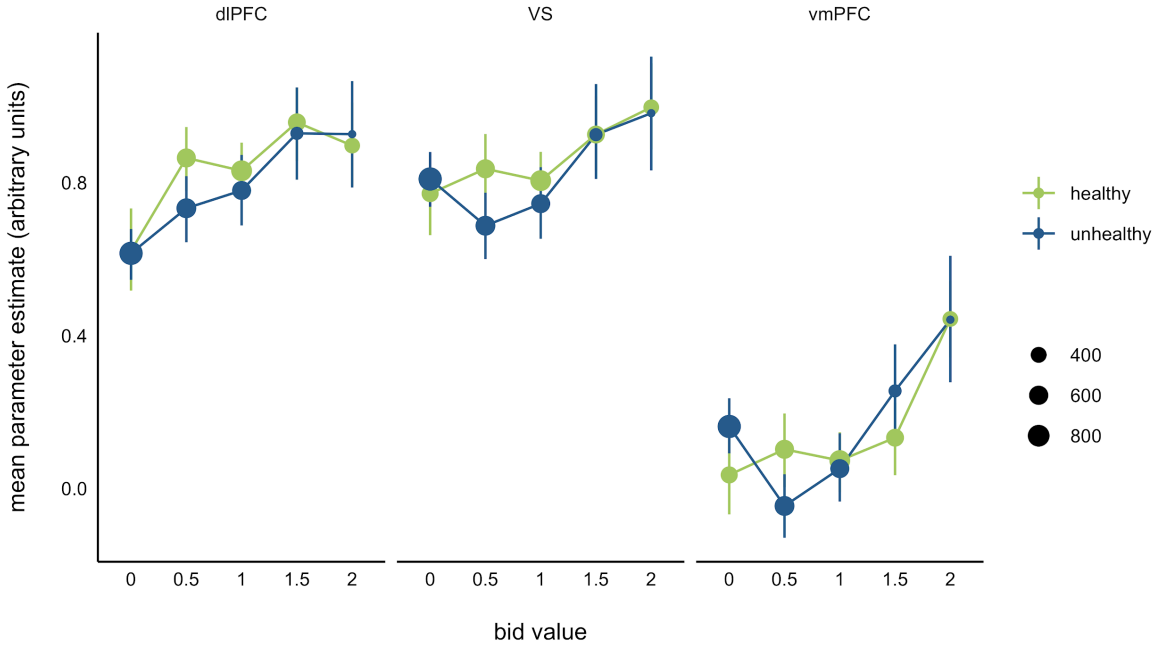

Figure 6. Mean parameter estimates of BOLD signal as a function of bid value, Food Type (healthy or unhealthy) and ROI. Points are scaled by the number of observations. Error bars are 95% confidence intervals across trials.

Model comparison

In general, results of the multilevel modeling analyses did not support the dual-process hypothesis. Compared to the base model that included only the fixed effect of Food Type, adding the difference term representing the relative activation of dlPFC and VS to the model DP1 did improve model fit as indicated by a statistically significant change in chi-square, $\chi^2(1) = 8.42$, $p = .004$ (see Table 2 for a summary of model fit results). However, the model that included an additional term for vmPFC activity (DP2) significantly improved fit over the basic dual-process model (DP1), $\chi^2(1) = 31.26$, $p < .001$. In DP2 (see Table 3), each one standard deviation increase in vmPFC activity was associated with a 5.0 cent increase in bid value ($b = 0.05$, 95% CI = [0.03, 0.06], $p < .001$), while the difference between dlPFC and VS activity was associated with a 1.8 cent increase for each SD change ($b = 0.02$, 95% CI = [0.00, 0.03], $p = .046$).

Table 2
Summary of Model Comparison Results

Model	*df*	χ2 (*df*)	AIC	Deviance	*p*
Dual-process models					
Base model	4	–	9753.22	9745.22	–
DP1	5	8.42 (1)	9746.80	9736.80	.004
DP2	6	31.26 (1)	9717.54	9705.54	< .001
Value-based choice models					
Base model	4	–	9753.22	9745.22	–
VB1	**7**	**53.73 (3)**	**9705.49**	**9691.49**	**< .001**

Note. Models were compared sequentially in the order presented here using a change in chi-square difference test. A statistically significant *p* value (i.e., $p < .05$) indicates that that model fits the data better than the model above. The **bolded model** is the best fitting model.

In contrast, results generally supported the hypotheses of the value-based choice model. Fit improved significantly from the base model when individual terms for dlPFC, vmPFC, and VS activity were added, according to the chi-square difference test, $\chi^2(3) = 53.73$, $p < .001$. Furthermore, directly comparing the canonical dual-process and value-based choice models

(DP1 and VB1, respectively) revealed the value-based choice model as the better fitting, AIC_{DP1} = 9746.80, R^2_{DP1} = .19, AIC_{VB1} = 9705.49, R^2_{VB1} = .20. Critically, VB1 was also the best fitting model compared to other, non-preregistered potential specifications of dual-process and value-based choice models (see specification curve in Supplementary material). Inspection of the fixed effects of the canonical value-based choice model (VB1) revealed that bid value was positively associated with dlPFC activity (b = 0.04, 95% CI = [0.02, 0.06], p < .001) and vmPFC activity (b = 0.03, 95% CI = [0.01, 0.05], p = .003). Each one standard deviation increase in dlPFC activity was associated with a 4.4 cent increase in bid value, whereas it was associated with a 3.1 cent increase for vmPFC. VS activity was not significantly associated with bid value, b = 0.00, 95% CI = [-0.02, 0.02], p = .950. See Table 3 for VB1 parameter estimates and statistics.

Table 3
Results of the Multilevel Models DP1, DP2, and VB1

		Fixed effects		
DP1	*b*	*SE*	*t (df)*	*p*
Intercept	**0.96**	**0.03**	**34.08 (106.04)**	**< .001**
Food Type	**-0.30**	**0.02**	**18.43 (5219.69)**	**< .001**
dlPFC - VS	**0.02**	**0.01**	**2.90 (5305.03)**	**.004**
		Random effects		
	variance	*SD*		
Participant	0.06	0.24		

		Fixed effects		
DP2	*b*	*SE*	*t (df)*	*p*
Intercept	**0.95**	**0.03**	**33.78 (106.18)**	**< .001**
Food Type	**-0.30**	**0.02**	**18.44 (5218.74)**	**< .001**
dlPFC - VS	0.02	0.01	2.00 (5305.17)	.046
vmPFC	**0.05**	**0.01**	**5.60 (5305.69)**	**< .001**
		Random effects		
	variance	*SD*		
Participant	0.06	0.24		

		Fixed effects		
VB1	*b*	*SE*	*t (df)*	*p*
Intercept	**0.92**	**0.03**	**31.34 (125.43)**	**< .001**

Food Type	**-0.30**	**0.02**	**18.25 (5218.31)**	**< .001**
dlPFC	**0.04**	**0.01**	**3.83 (5304.49)**	**< .001**
VS	0.00	0.01	0.06 (5301.72)	.950
vmPFC	**0.03**	**0.01**	**3.00 (5305.26)**	**.003**
		Random effects		
	variance	*SD*		
Participant	0.06	0.24		

Note. DP1 is the model representing the core dual-process theoretical model; DP2 adds a term for vmPFC to DP1; VB1 is the model representing the core value-based choice theoretical model. The reference group for Food Type is healthy. **Bolded values** indicate statistical significance at $p < .01$. Degrees of freedom (*df*) were calculated using the Satterthwaite approximation.

We also observed qualified support for vmPFC integrating responses from the dlPFC and VS, as hypothesized by the value-based choice model (see Table 4). The results of this multilevel model showed that both dlPFC ($b = 0.43$, 95% CI = [0.40, 0.46], $p < .001$) and VS ($b = 0.12$, 95% CI = [0.09, 0.14], $p < .001$) were positively associated with vmPFC activity, but their interaction was not ($b = 0.01$, 95% CI = [0.00, 0.02], $p = .123$).

Table 4
Results of the Multilevel Model Regressing vmPFC Activity on dlPFC and VS

Fixed effects	*b*	*SE*	*t (df)*	*p*
Intercept	**-0.32**	**0.04**	**7.69 (101.75)**	**< .001**
dlPFC	**0.43**	**0.01**	**29.75 (5306.36)**	**< .001**
VS	**0.12**	**0.01**	**8.08 (5306.96)**	**< .001**
dlPFC×VS	0.01	0.01	1.54 (5262.86)	.123
Random effects	variance	*SD*		
Participant	0.14	0.37		

Note. This model represents an ancillary hypothesis of value-based choice models, that the interaction between dlPFC and VS is associated with vmPFC activity. **Bolded values** indicate statistical significance at $p < .001$. Degrees of freedom (*df*) were calculated using the Satterthwaite approximation.

Discussion

We used a novel trial-by-trial statistical modeling approach to compare two prominent neurocognitive models of self-control. Analyses focused on the three ROIs (dlPFC, VS, and vmPFC) commonly implicated in dual-process and value-based choice models of self-control.

We preregistered and tested competing hypotheses about these regions posed by the theoretical models, then compared the models based on their fit to the data.

Our results did not support the core hypothesis posed by the dual-process model – that the relative activation between dlPFC and VS is what drives self-control relevant outcomes (Lopez et al., 2017). If this were the case, DP1 should have been the best fitting model, but it was not. In addition, the consistent improvement in fit when including vmPFC is inconsistent with dual-process theory. Though chi-square statistics are sensitive to the number of free parameters, the lack of evidence for the dual-process models is not merely a function of reduced degrees of freedom. Because we preregistered our models, parameters were not included or excluded based on chance variation in the data. Also, VB1 had the lowest AIC, which penalizes additional parameters to reduce overfitting, despite having the most model parameters. Therefore, these results are inconsistent with the hypothesis that self-control relevant decisions result from antagonism between dlPFC and VS.

In contrast, our results support the value-based choice hypothesis that vmPFC activity is associated with self-control relevant decisions. Including vmPFC improved model fit, and the value-based choice model, VB1, was the best fitting model overall. Further, activation in the two regions that putatively represent the value of relevant choice attributes in this context – health in dlPFC and taste in VS – were both positively related to vmPFC activation. The observed positive correlation between VS and dlPFC is more consistent with the value-based choice model, where multiple attributes can contribute to the value of an option simultaneously.

Together, these results have implications for translational interventions to improve self-control. For example, they suggest that interventions seeking to amplify the subjective value of food health and/or decrease the value of food taste (e.g., via cognitive reappraisal) may be more

effective than interventions targeting inhibitory control. Additionally, because the value-based choice model isn't limited to "hot" and "cold" choice attributes, this model suggests other sources of value, such as social norms or identity (Nook & Zaki, 2015; Berkman, Livingston, & Kahn, 2017; Pfeifer & Berkman, 2018), may be useful intervention targets.

However, our results did not support one secondary hypothesis of the value-based choice model. The model posed by Berkman and colleagues (2017) specifies that vmPFC integrates value signals from dlPFC and VS, but it is unclear exactly how this "integration" happens. If vmPFC merely serves to sum the weighted inputs, then an additive, "main effects only" model might be possible. If vmPFC performs a more complex calculation (e.g., input-contingent) then an interaction model might also be possible. Thus, we tested both possibilities. Contrary to our hypothesis, while VS and dlPFC were positively associated with vmPFC activity, their interaction was not. Though there is no consensus across the various formulations of value-based choice models as to whether or not there are interactions among the inputs to the value accumulation (Berkman et al., 2017; Hare, Malmaud, & Rangel, 2011; Lim et al., 2018; Sullivan et al., 2015), these data indicate that an interaction might not be present, at least in this task.

In light of the vmPFC model results, it is notable that this study design did not permit us to test directional relationships among ROIs. Though it would be possible to assess directionality using structural equation modeling, this method requires large samples (Kline, 2016) and we were underpowered to utilize it. Examining the structural relationship among these ROIs is an important avenue for future research. Previous tests of the directional relationship between vmPFC and dlPFC using a similar food task indicated that dlPFC moderated activity in vmPFC, which in turn influenced choice (Hare, Malmaud, & Rangel, 2011). The influence of dlPFC on

vmPFC value signals has also been observed in other contexts (Hare, Camerer, & Rangel, 2009; Hare, Hakimi, & Rangel, 2014).

The pattern of activity in VS is noteworthy in two ways. This region has been implicated in reward motivation (Kelley, 2004; Schultz et al., 1992), providing the basis of the dual-process prediction that VS activation would be more closely linked with bids for hedonically rewarding, unhealthy foods compared to healthy ones. In contrast, activity in VS was positively correlated with bid value regardless of stimulus type (see Figure 5). It is possible that VS can represent non-hedonic types of reward (such as health) when stimuli come to be associated with those rewards for some other reason (such as a dieting goal). At the same time, we observed a drop in the magnitude of the positive relation between bid value and VS activity when dlPFC activity was entered into the model. This reduction may be due to the collinearity between VS and dlPFC, which in turn might be attributable to the participants' dieting goals. Cases where participants choose between one option that has (mostly) hedonic value and another that has both abstract goal value and (at least some) hedonic value are understudied in the research literature but might more realistically reflect how self-control relevant decisions operate. Compared to dual-process models, value-based choice models can more flexibly account for these cases because the value-integration process is agnostic about the number and sign of value inputs to a choice. Only in value-based choice models can VS, presumably representing hedonic or immediate reward value of some kind, contribute positively toward *both* options in a choice.

This study has several limitations. First, we did not collect independent liking, health, or taste ratings. These ratings would be necessary to make claims about the engagement of self-control or the relative contributions of taste and health on any single trial. Instead, our approach was to induce self-control goal dilemmas by sampling dieters with healthy eating goals and

looking at average effects across participants to test neurocognitive models of self-control. Second, we used a bid increments of $0.50, which may limit power in studies with smaller sample sizes and/or fewer experimental trials (but see Simms et al., 2019). Finally, region-to-region differences in signal-to-noise ratio (SNR) can make it difficult to compare the relative contributions of various brain regions to a statistical model. Indeed, there were region-wise differences in SNR (see Supplementary material), but the vmPFC had the lowest SNR of the three focal regions, suggesting that SNR alone cannot account for the observed effects.

The primary contribution of this research is the first direct comparison of two neurocognitive models of self-control, but several other features of the study are also noteworthy. The ecological validity of the task was high because our participants were overweight dieters who were bidding on food they would actually receive. This feature of the study is in contrast to many studies in the self-control literature that use a convenience sample without necessarily verifying that they have goals (e.g., dieting) that would confer subjective value to the healthiness of a food (Milyavskaya, Berkman, & De Ridder, 2018). The translational value of the results stems in part from the fact that the most common target for weight-reducing interventions is precisely the population from which the sample is drawn – overweight people who want to diet.

This study also highlights the usefulness of studying self-control within the context of an actual goal, dieting, that has strong translational potential. Dieting is a promising model for self-control because it unfolds across a longer time span than a typical laboratory study – extending weeks or months as opposed to an hour – and yet consists of a series of individual decisions (i.e., food choices) that can be investigated with a brief laboratory session. The context of dieting can also be fruitful for informing models of self-control because it can imbue different types of

stimuli with value by increasing the importance of different attributes; for example, a slice of cake holds both (positive) hedonic value and, simultaneously (negative) value with respect to the dieting goal. Though our study design precluded a test of whether participants' valuation of snack foods changed across contexts, our data are consistent with the possibility that the *healthy* foods might have accumulated some hedonic value in addition to their health goal value. In this way, dieting provides a more nuanced, complex test of self-control theories by shifting and broadening the set of food attributes that are relevant to participants' multiple and (sometimes) competing goals.

Conclusions

We found the value-based choice model of self-control better described the observed data. Our results neither prove nor disprove the theories of self-control, but instead provide evidence in support of the predictions of this and similar value-based choice models that activity in vmPFC is related to decisions requiring self-control and is positively associated with dlPFC and VS. Contrary to predictions, we found evidence suggesting that dlPFC and VS are not interactively associated with vmPFC, and our study design could not clarify the directionality of the relationships among these regions. Nevertheless, our unique approach to modeling neuroimaging data on a trial-by-trial basis and comparing theoretical models has helped refine our understanding of the neurobiological mechanisms underlying self-control and may, in turn, help inform the development of translational interventions to aid those who struggle with self-control.

Author contributions

All authors developed the study concept and analytic plan. D. Cosme and R. M. Ludwig performed the data analysis and interpretation under the supervision of E. T. Berkman. D. Cosme

and R. M. Ludwig drafted the manuscript, and E. T. Berkman provided critical revisions. All authors approved the final version of the manuscript for submission.

Funding

This work was supported by the NIH (CA211224 and CA17524 to ETB, and CA232357 to DC).

Acknowledgements

We thank Nicole Giuliani for helping design the original study, Junaid Merchant and Bryce Dirks for data collection, and Dagmar Zeithamova for methodological consultation. Elliot Berkman is manager of Berkman Consultants, LLC.

References

Aho, K., Derryberry, D., & Peterson, T. (2014). Model selection for ecologists: the worldviews of AIC and BIC. *Ecology*, *95*(3), 631-636.

Bakdash, J. Z., & Marusich, L. R. (2017). Repeated measures correlation. *Frontiers in Psychology*, *8*, 456.

Bartra, O., McGuire, J. T., & Kable, J. W. (2013). The valuation system: a coordinate-based meta-analysis of BOLD fMRI experiments examining neural correlates of subjective value. *Neuroimage*, *76*, 412-427.

Bates D., Mächler M., Bolker B., Walker S. (2015). Fitting linear mixed-effects models using lme4. *Journal of Statistical Software*, *67*(1), 1–48.

Berkman, E.T. (2017). The neuroscience of self-control. In D. de Ridder, M. Adriaanse, & K. Fujita (Eds.), *Handbook of Self-Control in Health and Wellbeing* (pp. 112-124). Abingdon-on-Thames: Routledge.

Berkman, E. T., Hutcherson, C. A., Livingston, J. L., Kahn, L. E., & Inzlicht, M. (2017). Self-control as value-based choice. *Current Directions in Psychological Science*, *26*(5), 422-428.

Berkman, E. T., Livingston, J. L., & Kahn, L. E. (2017). Finding the "self" in self-regulation: The identity-value model. *Psychological Inquiry*, *28*(2-3), 77-98.

Braver, T. S., Paxton, J. L., Locke, H. S., & Barch, D. M. (2009). Flexible neural mechanisms of cognitive control within human prefrontal cortex. Proceedings of the National Academy of Sciences, 106(18), 7351-7356.

Buhle, J. T., Silvers, J. A., Wager, T. D., Lopez, R., Onyemekwu, C., Kober, H., ... & Ochsner, K. N. (2014). Cognitive reappraisal of emotion: a meta-analysis of human neuroimaging studies. Cerebral cortex, 24(11), 2981-2990.

Clithero, J. A., & Rangel, A. (2013). Informatic parcellation of the network involved in the computation of subjective value. *Social Cognitive and Affective Neuroscience*, *9*(9), 1289-1302.

Cosme, D., Flournoy, J. C., & DeStasio, K. L. (2018). Auto-motion [Code repository]. Retrieved from http://doi.org/10.5281/zenodo.1240528

Cox, R. W. (1996). AFNI: software for analysis and visualization of functional magnetic resonance neuroimages. *Computers and Biomedical Research*, *29*(3), 162-173.

Desikan, R. S., Ségonne, F., Fischl, B., Quinn, B. T., Dickerson, B. C., Blacker, D., ... & Albert, M. S. (2006). An automated labeling system for subdividing the human cerebral cortex on MRI scans into gyral based regions of interest. *Neuroimage*, *31*(3), 968-980.

Destrieux, C., Fischl, B., Dale, A., & Halgren, E. (2010). Automatic parcellation of human cortical gyri and sulci using standard anatomical nomenclature. *Neuroimage*, *53*(1), 1-15.

Duncan, J. (2013). The structure of cognition: attentional episodes in mind and brain. Neuron, 80(1), 35-50.

Figner, B., Knoch, D., Johnson, E. J., Krosch, A. R., Lisanby, S. H., Fehr, E., & Weber, E. U. (2010). Lateral prefrontal cortex and self-control in intertemporal choice. *Nature Neuroscience*, *13*(5), 538.

Fischl, B. (2012). FreeSurfer. *Neuroimage*, *62*(2), 774-781.

Fischl, B., Salat, D. H., Busa, E., Albert, M., Dieterich, M., Haselgrove, C., ... & Montillo, A. (2002). Whole brain segmentation: automated labeling of neuroanatomical structures in the human brain. *Neuron*, *33*(3), 341-355.

Fujita, K. (2011). On conceptualizing self-control as more than the effortful inhibition of impulses. Personality and Social Psychology Review, 15(4), 352-366.

Fujita, K., Carnevale, J. J., & Trope, Y. (2018). Understanding self-control as a whole vs. part dynamic. *Neuroethics*, *11*(3), 283-296.

Hare, T. A., Camerer, C. F., Knoepfle, D. T., O'Doherty, J. P., & Rangel, A. (2010). Value computations in ventral medial prefrontal cortex during charitable decision making incorporate input from regions involved in social cognition. *Journal of Neuroscience*, *30*(2), 583-590.

Hare, T. A., Camerer, C. F., & Rangel, A. (2009). Self-control in decision-making involves modulation of the vmPFC valuation system. *Science*, *324*(5927), 646-648.

Hare, T. A., Hakimi, S., & Rangel, A. (2014). Activity in dlPFC and its effective connectivity to vmPFC are associated with temporal discounting. *Frontiers in Neuroscience*, *8*, 50.

Hare, T. A., Malmaud, J., & Rangel, A. (2011). Focusing attention on the health aspects of foods changes value signals in vmPFC and improves dietary choice. *Journal of Neuroscience*, *31*(30), 11077-11087.

Harris, A., Clithero, J. A., & Hutcherson, C. A. (2018). Accounting for taste: A multi-attribute neurocomputational model explains the neural dynamics of choices for self and others. *Journal of Neuroscience*, *38*(37), 7952-7968.

Heatherton, T. F., & Wagner, D. D. (2011). Cognitive neuroscience of self-regulation failure. Trends in cognitive sciences, 15(3), 132-139.

Hutcherson, C. A., Plassmann, H., Gross, J. J., & Rangel, A. (2012). Cognitive regulation during decision making shifts behavioral control between ventromedial and dorsolateral prefrontal value systems. *Journal of Neuroscience*, *32*(39), 13543-13554.

Jenkinson, M., Beckmann, C. F., Behrens, T. E., Woolrich, M. W., & Smith, S. M. (2012). Fsl. *Neuroimage*, *62*(2), 782-790.

Kelley, A. E. (2004). Ventral striatal control of appetitive motivation: role in ingestive behavior and reward-related learning. *Neuroscience & Biobehavioral Reviews*, *27*(8), 765-776.

Kline, R. B. (2016). *Methodology in the social sciences. Principles and practice of structural equation modeling (4th ed).* New York, NY, US: Guilford Press.

Kotabe, H. P., & Hofmann, W. (2015). On integrating the components of self-control. *Perspectives on Psychological Science*, *10*(5), 618-638.

Levy, D. J., & Glimcher, P. W. (2012). The root of all value: a neural common currency for choice. *Current Opinion in Neurobiology*, *22*(6), 1027-1038.

Lieberman, M. D., Straccia, M. A., Meyer, M. L., Du, M., & Tan, K. M. (2019). Social, self,(situational), and affective processes in medial prefrontal cortex (MPFC): Causal, multivariate, and reverse inference evidence. *Neuroscience & Biobehavioral Reviews*.

Lim, S. L., O'Doherty, J. P., & Rangel, A. (2011). The decision value computations in the vmPFC and striatum use a relative value code that is guided by visual attention. *Journal of Neuroscience*, *31*(37), 13214-13223.

Lim, S. L., Penrod, M. T., Ha, O. R., Bruce, J. M., & Bruce, A. S. (2018). Calorie labeling promotes dietary self-control by shifting the temporal dynamics of health-and taste-attribute integration in overweight individuals. *Psychological Science*, *29*(3), 447-462.

Lopez, R. B., Chen, P. H. A., Huckins, J. F., Hofmann, W., Kelley, W. M., & Heatherton, T. F. (2017). A balance of activity in brain control and reward systems predicts self-regulatory outcomes. *Social Cognitive and Affective Neuroscience*, *12*(5), 832-838.

Lopez, R. B., Hofmann, W., Wagner, D. D., Kelley, W. M., & Heatherton, T. F. (2014). Neural predictors of giving in to temptation in daily life. Psychological science, 25(7), 1337-1344.

Lorah, J. (2018). Effect size measures for multilevel models: definition, interpretation, and TIMSS example. *Large-scale Assessments in Education*, *6*(1), 8.

MacDonald, A. W., Cohen, J. D., Stenger, V. A., & Carter, C. S. (2000). Dissociating the role of the dorsolateral prefrontal and anterior cingulate cortex in cognitive control. Science, 288(5472), 1835-1838.

McClure, S. M., Ericson, K. M., Laibson, D. I., Loewenstein, G., & Cohen, J. D. (2007). Time discounting for primary rewards. *Journal of Neuroscience*, *27*(21), 5796-5804.

Miller, E. K., & Cohen, J. D. (2001). An integrative theory of prefrontal cortex function. Annual review of neuroscience, 24(1), 167-202.

Milyavskaya, M., Berkman, E. T., & De Ridder, D. T. (2019). The many faces of self-control: Tacit assumptions and recommendations to deal with them. *Motivation Science*, *5*(1), 79.

Nook, E. C., & Zaki, J. (2015). Social norms shift behavioral and neural responses to foods. *Journal of Cognitive Neuroscience*, *27*(7), 1412-1426.

Padoa-Schioppa, C., & Conen, K. E. (2017). Orbitofrontal cortex: A neural circuit for economic decisions. *Neuron*, *96*(4), 736-754.

Pfeifer, J. H., & Berkman, E. T. (2018). The Development of Self and Identity in Adolescence: Neural Evidence and Implications for a Value-Based Choice Perspective on Motivated Behavior. *Child Development Perspectives*, *12*(3), 158-164.

Plassmann, H., O'Doherty, J. P., & Rangel, A. (2010). Appetitive and aversive goal values are encoded in the medial orbitofrontal cortex at the time of decision making. *Journal of Neuroscience*, *30*(32), 10799-10808.

Rangel, A., & Hare, T. (2010). Neural computations associated with goal-directed choice. *Current Opinion in Neurobiology*, *20*(2), 262-270.

Rissman, J., Gazzaley, A., & D'Esposito, M. (2004). Measuring functional connectivity during distinct stages of a cognitive task. *Neuroimage*, *23*(2), 752-763.

Roy, M., Shohamy, D., & Wager, T. D. (2012). Ventromedial prefrontal-subcortical systems and the generation of affective meaning. *Trends in Cognitive Sciences*, *16*(3), 147-156.

Schultz, W., Apicella, P., Scarnati, E., & Ljungberg, T. (1992). Neuronal activity in monkey ventral striatum related to the expectation of reward. *Journal of Neuroscience*, *12*(12), 4595-4610.

Shenhav, A. (2017). The perils of losing control: Why self-control is not just another value-based decision. *Psychological Inquiry*, *28*(2-3), 148-152.

Shenhav, A., Botvinick, M. M., & Cohen, J. D. (2013). The expected value of control: an integrative theory of anterior cingulate cortex function. Neuron, 79(2), 217-240.

Simms, L. J., Zelazny, K., Williams, T. F., & Bernstein, L. (2019). Does the number of response options matter? Psychometric perspectives using personality questionnaire data. Psychological assessment, 31(4), 557.

Simonsohn, U., Simmons, J. P., & Nelson, L. D. (2015). Specification Curve: Descriptive and Inferential Statistics on All Reasonable Specifications. *SSRN Electronic Journal*. https://doi.org/10.2139/ssrn.2694998

Sullivan, N., Hutcherson, C., Harris, A., & Rangel, A. (2015). Dietary self-control is related to the speed with which attributes of healthfulness and tastiness are processed. *Psychological Science*, *26*(2), 122-134.

Tusche, A., & Hutcherson, C. A. (2018). Cognitive regulation alters social and dietary choice by changing attribute representations in domain-general and domain-specific brain circuits. *eLife*, *7*, e31185.

Yarkoni, T., Poldrack, R. A., Nichols, T. E., Van Essen, D. C., & Wager, T. D. (2011). Large-scale automated synthesis of human functional neuroimaging data. *Nature Methods*, *8*(8), 665.

Supplementary material

Participant enrollment exclusion criteria

All participants were right-handed, native English speakers, and were screened for MRI eligibility. MRI exclusion criteria included metal implants (e.g., braces, pins), embedded metal fragments, biomedical devices (e.g., pacemakers, cochlear implants), claustrophobia, and risk for pregnancy. In order to reduce confounds, participants were also excluded if they were currently diagnosed with a neurological, psychiatric, or eating disorder, or are taking psychotropic medications. Due to the physical constraints of the MRI machine, only participants weighing less than 500 lbs. were included. Further, as the intervention was administered via text message and some surveys were completed at home, only participants with cell phones and internet access were included.

Neuroimaging scan sequence parameters

We acquired a high-resolution anatomical T1-weighted MP-RAGE scan (TR/TE = 2500.00/3.43ms, 256 × 256 matrix, 1mm thick, 176 sagittal slices, FOV = 208 × 208mm), functional images with a T2*- weighted echo-planar sequence (72 axial slices, TR/TE = 2000.00/26.00ms, 90-degree flip angle, 104 × 104 matrix, 2mm thick, FOV = 208 × 208mm), and opposite phase encoded echo-planar images to correct for magnetic field inhomogeneities (72 axial slices, TR/TE = 6390.00/47.80ms, 90-degree flip angle, 104 ×104 matrix, 2mm thick, FOV = 208 × 208mm).

ROI definition

For the analyses reported in the main text, we determined which cortical parcels to use by inspecting meta-analytic association test maps from NeuroSynth (Yarkoni et al., 2011) and identifying overlapping parcels in FreeSurfer (see Figure S1). To create the dlPFC ROI, we

concatenated the bilateral middle frontal gyrus (aparc2009 parcels: 11115, 12115) and the inferior frontal sulcus (aparc2009 parcels: 11153, 12153) parcels. We created the vmPFC ROI using the medial orbitofrontal cortex parcels (aparc parcels: 1014, 2014) and the VS ROI by concatenating the nucleus accumbens (aseg segments: 26, 58) and putamen (aseg segments: 12, 51) segments.

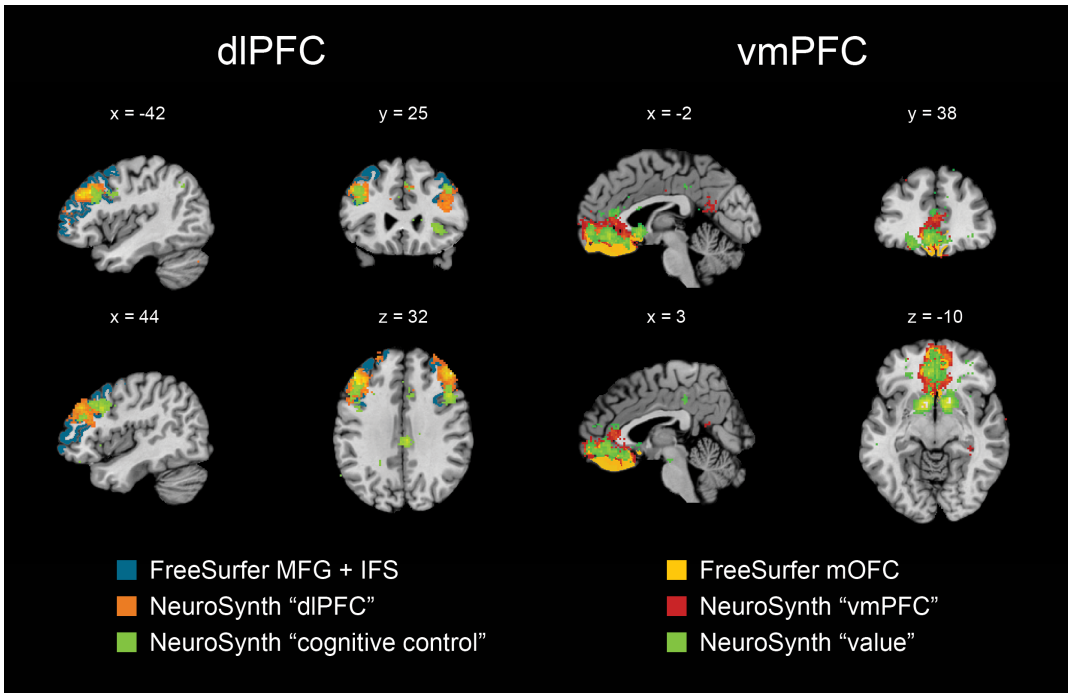

Figure S1. ROIs were defined by identifying which parcels in FreeSurfer parcellation atlases overlapped with relevant meta-analytic association test maps from NeuroSynth. dlPFC = dorsolateral prefrontal cortex, vmPFC = ventromedial prefrontal cortex, MFG = middle frontal gyrus, IFS = inferior frontal sulcus, mOFC = medial orbitofrontal cortex.

Specification curve analysis

We constructed and preregistered the dual-process and value-based choice models reported in the main manuscript based on our interpretation of the literature. However, we recognize that these are two specifications (i.e., DP1 and VB1) among many others that might have been specified. Therefore, we specified additional possible instantiations of dual-process and value-based choice models and compared model fit using a specification curve (Simonsohn,

Simmons, & Nelson, 2015; see Figure S2). Of the models compared, the best fitting model reported in the main manuscript (VB1/specification 1) remains the best fitting model even when compared to other competing specifications.

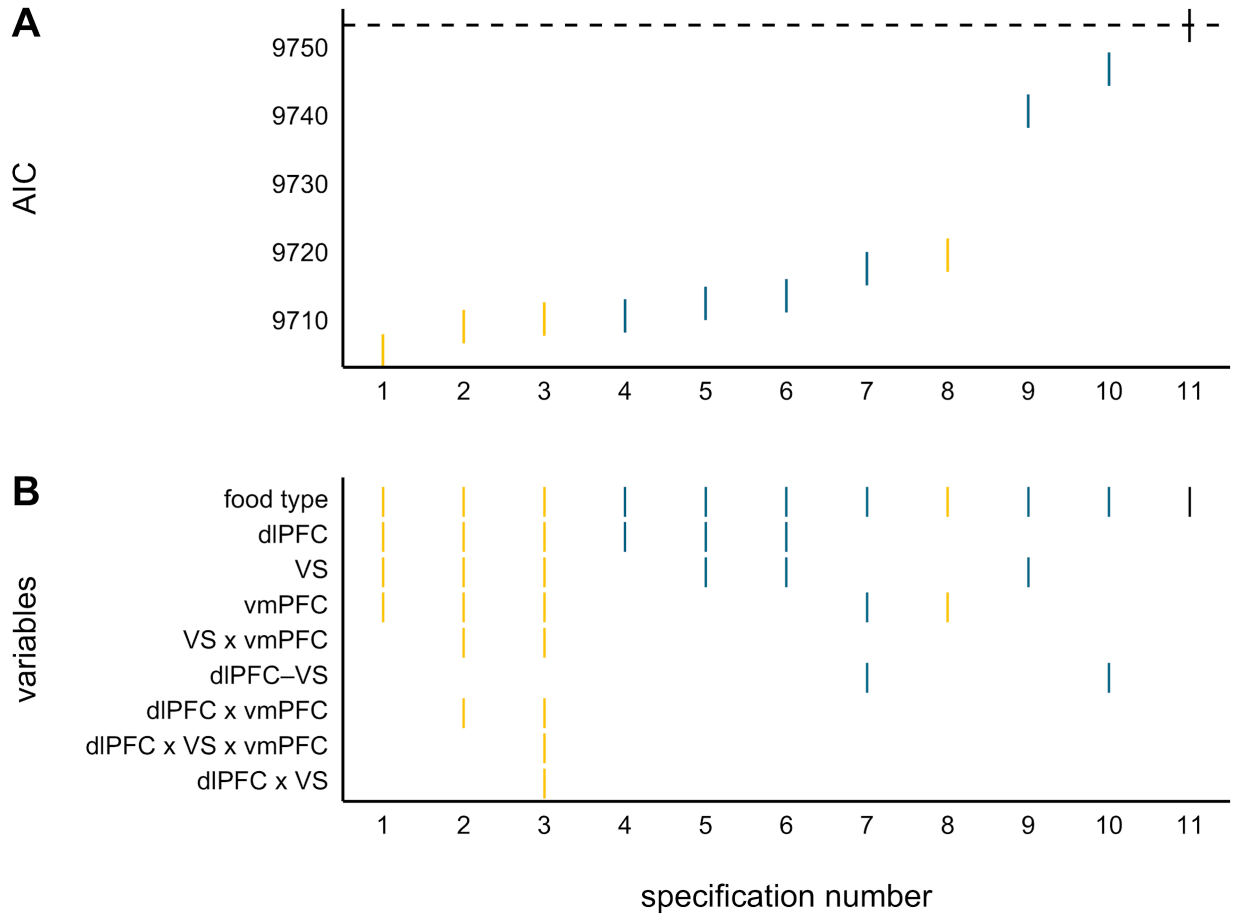

Figure S2. Specification curve analysis of 11 unique models ordered based on model fit (AIC). Each column corresponds to a single model specification. The AIC value for each model specification is plotted in panel A and the variables included in each model are visualized in panel B. The base model, which included Food Type (healthy or unhealthy) as the only predictor, is visualized in black and the dotted black line represents the AIC for this model. Models construed as potential instantiations of dual-process models are visualized in blue, whereas instantiations of value-based choice models are in yellow. Specification 1 corresponds to VB1 and specification 10 corresponds to DP1 in the main manuscript. dlPFC = dorsolateral prefrontal cortex, VS = ventral striatum, vmPFC = ventromedial prefrontal cortex, dlPFC - VS = balance score between dlPFC and VS.

Specificity analyses

In our primary analyses, we chose to focus specifically on dlPFC and VS because these regions are most frequently implicated in neurocognitive models of self-control. However, we acknowledge that other regions (e.g., ventrolateral prefrontal cortex) may play a role in self-control as well. For example, other studies have averaged BOLD signal across multiple ROIs in the frontoparietal control and valuation networks rather than selecting singular canonical regions to represent each process (Lopez et al., 2017). To explore the specificity of the effects reported in the main text, we conducted two supplementary multilevel modeling analyses, outlined in our preregistration (addendum 2).

First, we repeated the model comparisons reported in the main text but with larger dlPFC and VS ROIs that included other relevant regions. Specifically, we created a lateral prefrontal cortex (lPFC) ROI by concatenating the following bilateral parcels from the Desikan-Killiany (Desikan et al., 2006) and Destrieux (Destrieux et al., 2010) cortical parcellation atlases: middle frontal gyrus (MFG), inferior frontal sulcus (IFS), pars opercularis, and pars triangularis. We created a striatum ROI by concatenating the bilateral nucleus accumbens (NAcc), putamen, and caudate segments using the segmentation atlas (Fischl et al., 2002) in FreeSurfer 6 (Fischl, 2012). We then ran the multilevel models but with lPFC and striatum, rather than dlPFC and VS.

The performance of these multilevel models mirrored those reported in the main text; that is, the value-based choice model was the best fitting model and the dual-process hypothesis was not supported. According to the chi-square difference test, the dual-process model that included a term for the difference between lPFC and striatum (DP1) did not significantly improve fit over the base model that contained only a term for Food Type (healthy or unhealthy), $\chi^2(1) = 2.83$, $p = .093$. However, a model that included an additional term for the vmPFC ROI (DP2) did

significantly improve fit over the former two models, $\chi^2(1) = 34.32$, $p < .001$. As before, the theoretical value-based choice model (VB1) significantly improved fit over the base model, $\chi^2(3) = 43.80$, $p < .001$. This model was also a better fitting model, $\chi^2(1) = 6.65$, $p = .010$, compared to the dual-process model with terms included for the difference between the lPFC and striatum and the vmPFC (DP2). Directly comparing the two theoretical models using the Akaike Information Criterion (AIC) again revealed that the value-based choice model was the best-fitting, $AIC_{DP1} = 9752.39$, $AIC_{VB1} = 9715.42$. Inspection of the fixed effects in the value-based choice model showed that of the neural regions, both lPFC ($b = 0.03$, $p = .021$) and vmPFC ($b = 0.04$, $p < .001$) were significantly associated with bid value, whereas the striatum was not ($b = 0.00$, $p = .979$), replicating the results from our primary ROIs of interest (see Table S1). Finally, we found that while activity in lPFC ($b = 0.38$, $p < .001$) and striatum ($b = 0.18$, $p < .001$) was positively associated with activity in vmPFC, the interaction between the two was not ($b = 0.01$, $p = .340$); see Table S2.

Table S1
Results of the Multilevel Models DP1, DP2, and VB1

		Fixed effects		
DP1	*b*	*SE*	*t (df)*	*p*
Intercept	**0.81**	**0.03**	**30.02 (89.02)**	**< .001**
Food Type	**0.15**	**0.01**	**18.44 (5219.69)**	**< .001**
lPFC - Striatum	0.02	0.01	1.68 (5306.60)	.093
		Random effects		
	variance	*SD*		
Participant	0.06	0.24		

		Fixed effects		
DP2	*b*	*SE*	*t (df)*	*p*
Intercept	**0.80**	**0.03**	**29.72 (89.24)**	**< .001**
Food Type	**0.15**	**0.01**	**18.45 (5218.74)**	**< .001**
lPFC - Striatum	0.01	0.01	1.21 (5305.92)	.227
vmPFC	**0.05**	**0.01**	**5.87 (5305.02)**	**< .001**

	Random effects	
	variance	*SD*
Participant	0.06	0.24

	Fixed effects			
VB1	*b*	*SE*	*t (df)*	*p*
Intercept	**0.78**	**0.03**	**27.84 (103.65)**	**< .001**
Food Type	**0.15**	**0.01**	**18.32 (5218.25)**	**< .001**
lPFC	**0.03**	**0.01**	**2.31 (5304.55)**	**.021**
Striatum	0.00	0.01	0.03 (5303.64)	.979
vmPFC	**0.04**	**0.01**	**3.68 (5304.48)**	**< .001**

	Random effects	
	variance	*SD*
Participant	0.06	0.24

Note. VB1 is the model representing the core value-based choice theoretical model; DP2 adds a term for vmPFC to the core dual-process theoretical model. The reference group for Food Type is healthy. **Bolded values** indicate statistical significance at $p < .05$. Degrees of freedom (*df*) were calculated using the Satterthwaite approximation.

Table S2

Results of the Multilevel Model Regressing vmPFC Activity on lPFC and Striatum

Fixed effects	*b*	*SE*	*t (df)*	*p*
Intercept	**-0.33**	**0.04**	**7.68 (100.40)**	**< .001**
lPFC	**0.38**	**0.02**	**22.81 (5306.02)**	**< .001**
Striatum	**0.18**	**0.02**	**10.65 (5306.41)**	**< .001**
lPFC×Striatum	0.01	0.01	0.95 (5258.34)	.340

Random effects	variance	*SD*
Participant	0.14	0.38

Note. This model represents an ancillary hypothesis of value-based choice models, that the interaction between lPFC and striatum is associated with vmPFC activity. **Bolded values** indicate statistical significance at $p < .001$. Degrees of freedom (*df*) were calculated using the Satterthwaite approximation.

Next, we explored the relationship between ROIs and bid values at a more fine-grained level by regressing bid value on Food Type and the following individual ROIs (i.e., not concatenated together): MFG, IFS, pars opercularis, pars triangularis, NAcc, putamen, caudate, and vmPFC. We chose to do this as it was conceptually impractical to use these smaller ROIs to construct a difference measure consistent with that theoretically specified by the dual-process model. Compared to the base model that included Food Type only, a model that included all of

the small ROIs except vmPFC did significantly improve fit to the data according to the chi-square difference test, $\chi^2(7) = 74.62$, $p < .001$. Again we found that including an ROI for vmPFC further improved model fit, $\chi^2(1) = 15.51$, $p < .001$. Interpreting the fixed effects from this best fitting model revealed that four ROIs were significantly associated with bid value: MFG ($b = 0.07$, $p < .001$), IFS ($b = 0.03$, $p < .001$), pars triangularis ($b = -0.08$, $p < .001$), and vmPFC ($b = 0.04$, $p < .001$). In addition to showing that MFG and IFS were independently related to bid value, these results further support the notion that vmPFC plays a role in dietary decisions that require self-control. In addition, results show that pars triangularis, which is frequently implicated in inhibitory control, was also associated with bid value, albeit negatively. Full results can be found in Table S3.

Table S3
Results of the Multilevel Model Regressing Bid Value on Food Type and ROIs

Fixed effects	*b*	*SE*	*t (df)*	*p*
Intercept	**0.76**	**0.03**	**26.25 (119.28)**	**< .001**
Food Type	**0.15**	**0.01**	**18.07 (5214.84)**	**< .001**
MFG	**0.07**	**0.02**	**4.42 (5156.80)**	**< .001**
IFS	**0.03**	**0.02**	**2.16 (5211.77)**	**.031**
Pars opercularis	0.01	0.02	0.29 (5294.46)	.774
Pars triangularis	**-0.08**	**0.02**	**4.96 (5297.98)**	**< .001**
NAcc	0.00	0.01	0.14 (5300.91)	.887
Putamen	0.01	0.01	1.18 (5290.88)	.237
Caudate	-0.01	0.01	k0.87 (5291.09)	.387
vmPFC	**0.04**	**0.01**	**3.94 (5300.92)**	**< .001**

Random effects	variance	*SD*
Participant	0.06	0.24

Note. The reference group for Food Type is healthy. **Bolded values** indicate statistical significance at $p < .05$. Degrees of freedom (*df*) were calculated using the Satterthwaite approximation.

Signal-to-noise ratio in ROIs

To verify that our results were not simply due to differences in the signal-to-noise ratio (SNR) among the ROIs, we computed temporal SNR for each participant's beta-series and

compared the mean temporal SNR and standard deviation (across voxels) in each ROI using the AFNI 3dTstat -tsnr command. The primary concern is that cortical ROIs have greater SNR and will therefore have an "advantage" above subcortical ROIs.

The results showed that there were differences both with respect to mean temporal SNR and variability in temporal SNR across voxels in each ROI (Figure S3). dlPFC had the highest mean temporal SNR (M = 0.39, SD = 0.10), followed by VS (M = 0.32, SD = 0.07), then vmPFC (M = 0.27, SD = 0.04). Pairwise t-tests showed that the temporal SNR in dlPFC was significantly higher than vmPFC (M_{diff} = 0.12, $t(89) = 14.06$, $p < .001$) and VS (M_{diff} = 0.07, $t(89) = 8.91$, $p < .001$), and it was significantly higher in VS than vmPFC (M_{diff} = 0.05, $t(89) = 7.10$, $p < .001$).

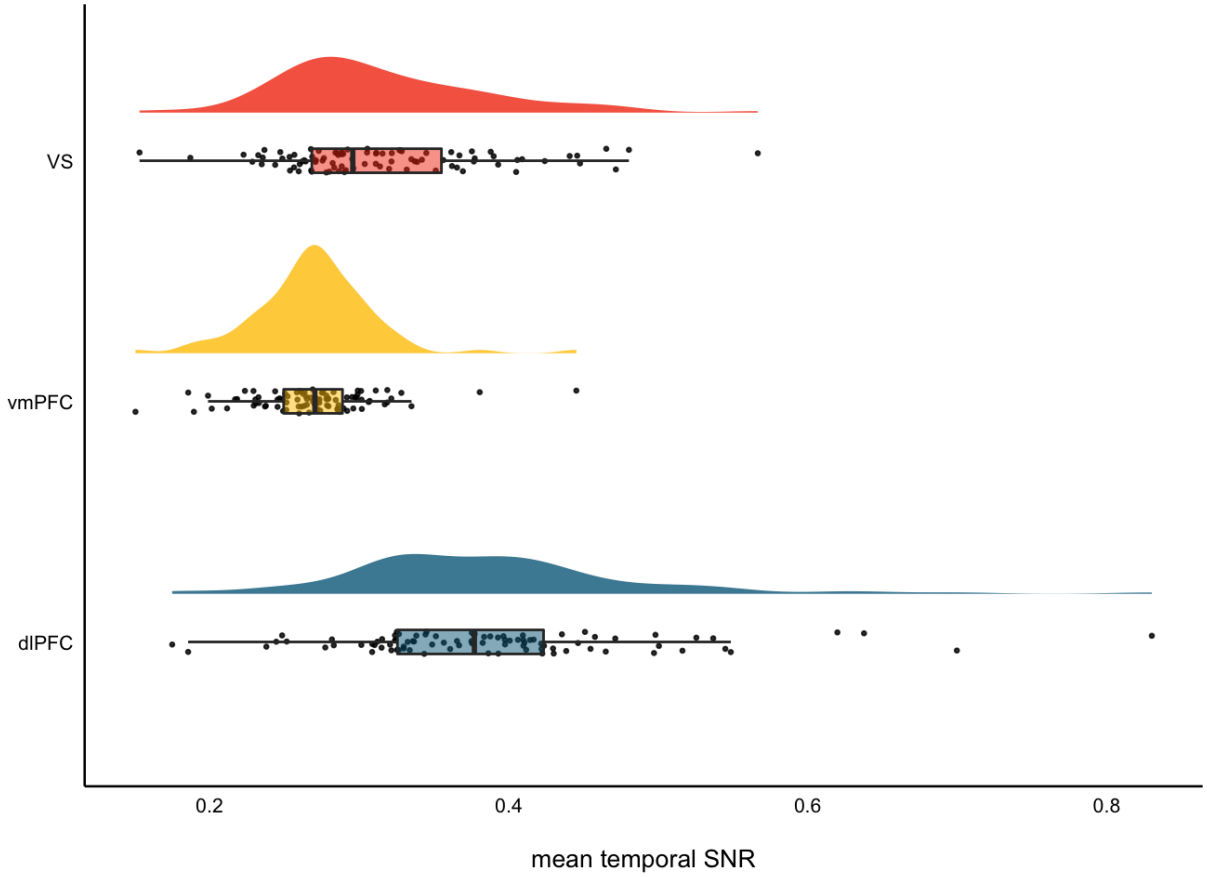

Figure S3. Mean temporal signal-to-noise ratio (SNR) among ROIs. Each dot represents a participant; temporal SNR was calculated across beta-series images for each participant separately.

The same pattern of results emerged for variability in temporal SNR across voxels in each ROI (Figure S4; dlPFC $M = 0.30$, $SD = 0.07$; VS $M = .0.23$, $SD = 0.05$; vmPFC $M = 0.21$, $SD = 0.04$). Pairwise t-tests showed that the temporal SNR variability across voxels in dlPFC was significantly higher than vmPFC ($M_{diff} = 0.09$, $t(89) = 17.34$, $p < .001$) and VS ($M_{diff} = 0.07$, $t(89) = 11.87$, $p < .001$), and it was significantly higher in VS than vmPFC ($M_{diff} = 0.03$, $t(89) = 6.94$, $p < .001$).

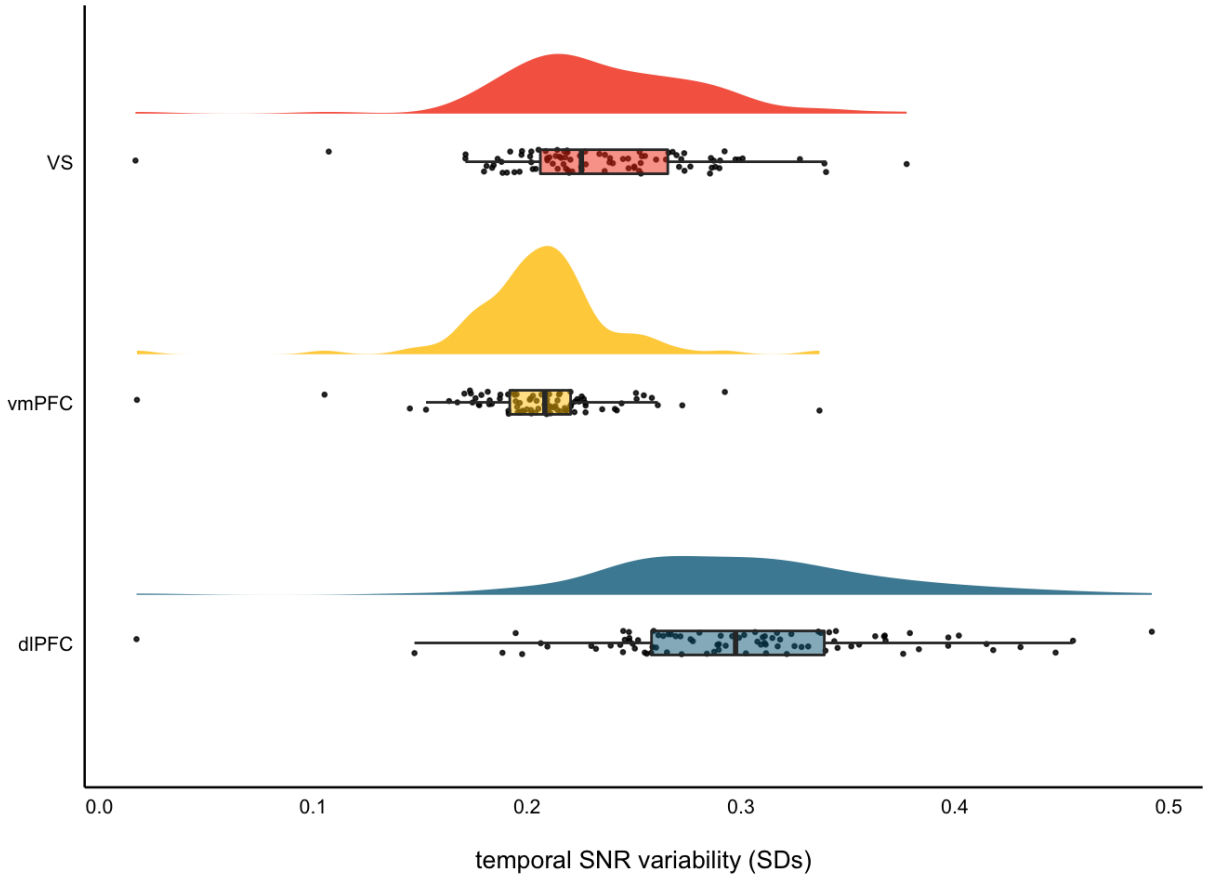

Figure S4. Mean temporal signal-to-noise ratio (SNR) variability across voxels in standard deviations within each ROI. Each dot represents a participant; temporal SNR was calculated across beta-series images for each participant separately.

Though these results provide important information for researchers conducting alternative modeling approaches using fMRI data, they do not invalidate the results presented in

the main manuscript. First, vmPFC had the lowest mean temporal SNR but was consistently associated with bid value and improved model fit when included. Second, it is notable that the difference score between dlPFC and VS may be affected by differences in temporal SNR, potentially limiting the strength of the inferences that can be made about the associated term in the model. However, there is substantial variability in the differences in temporal SNR between subjects and (Figure S5) and the implications of the magnitude of the effect (i.e., M_{diff} = 0.07) on bid values is unclear. Finally, our primary analyses do not hinge on direct comparisons between regions (e.g., by comparing beta weights) but rather between models. In this case as well, differences in SNR alone cannot account for the results because the region with the greatest SNR (dlPFC) appears in statistical models corresponding to dual-process models of self-control.

Nevertheless, the research presented in this manuscript would benefit from replication. In particular, a replication based on data from several MRI scanners with different sequence parameters known to affect signal-to-noise ratio would be particularly valuable because it could address the lingering question of how strongly the results are impacted by variance in signal-to-noise across the brain. Replication would also help estimate effect sizes more precisely. We hope this paper provides a blueprint for future replications in order to more thoroughly test the model predictions of dual-process and value-based choice models of self-control.

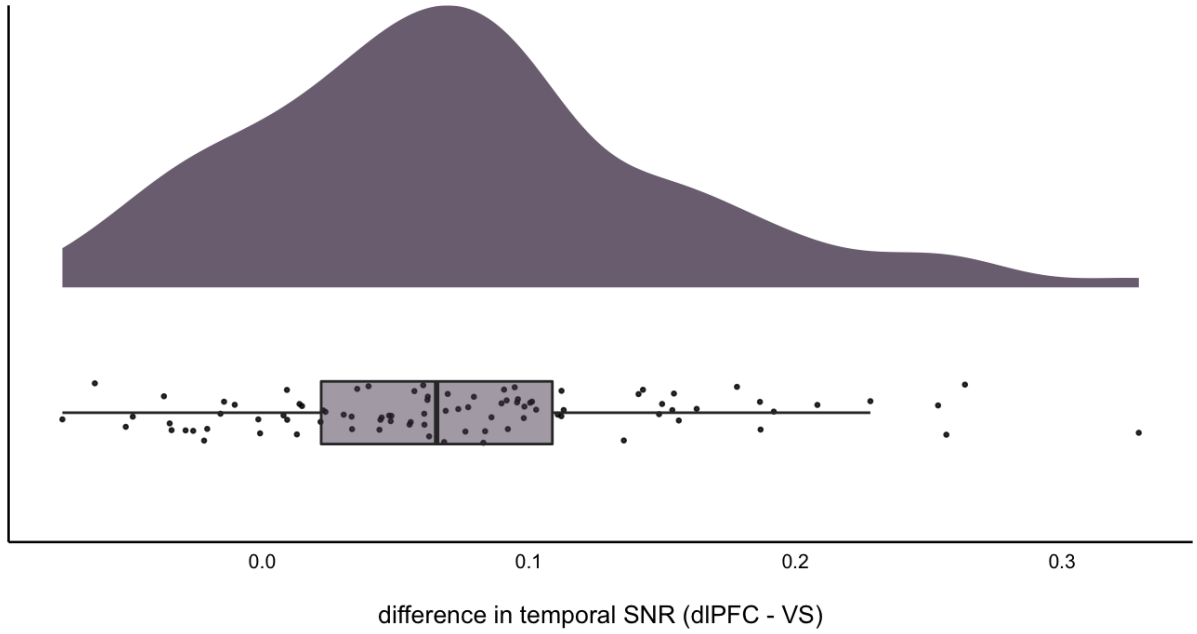

Figure S5. Difference in mean temporal signal-to-noise ratio (SNR) between dlPFC and VS. Each dot represents a participant; temporal SNR was calculated across beta-series images for each participant separately.